Journal of Functional Foods 105 (2023) 105566

Contents lists available at ScienceDirect

Journal of Functional Foods

journal homepage: www.elsevier.com/locate/jff

Effects of grape seed proanthocyanidin extract on lipopolysaccharide translocation and trafficking from the gut to tissues

Marta Sierra-Cruz [a], Alba Miguéns-Gómez [a], Esther Rodríguez-Gallego [a], Claudio D'Addario [b], Martina Di Bartolomeo [b], M Teresa Blay [a], Montserrat Pinent [a], Raúl Beltrán-Debón [a,*], Ximena Terra [a]

[a] Universitat Rovira i Virgili, Departament de Bioquímica i Biotecnologia, MoBioFood Research Group, Tarragona, Spain
[b] Faculty of Bioscience, University of Teramo, Teramo, Italy

ARTICLE INFO

Keywords:
Intestinal permeability
Metabolic endotoxemia
Proanthocyanidins
Gut microbiota
Systemic inflammation

ABSTRACT

Diet-associated alterations of the intestinal barrier and gut microbiota promote intestinal lipopolysaccharide (LPS) translocation from the lumen to the lamina propria through different pathways, leading to an increase in LPS levels in the plasma known as metabolic endotoxemia.

As a pharmacological dose of grape seed proanthocyanidin extract (GSPE) can reduce metabolic endotoxemia of obese rats, in the current study, we aimed to evaluate GSPE modulation of LPS translocation and the underlying mechanisms. We performed both an *in vitro* experiment with Caco-2 cells and an *in vivo* experiment with Wistar female rats fed a cafeteria (CAF) diet. GSPE was effective in regulating intestinal permeability through the modulation of receptor-mediated endocytosis pathway, as well as the gut microbiota interaction with the endocannabinoid system through epigenetic mechanisms. Our results confirm that GSPE can ameliorate intestinal dysfunction and metabolic endotoxemia caused by an excess of dietary lipids by modulating the endotoxin-translocation pathways.

1. Introduction

The gastrointestinal tract is a high-surface organ of the body. Its primary function is nutrient absorption but it is also a selective barrier and is involved in the immune defence, metabolism and endocrine functions (Ge et al., 2000; Gil-Cardoso et al., 2017).

Dietary pattern is a relevant factor affecting gut homeostasis. Under healthy dietary conditions, the intestinal barrier prevents the passage of undesirable compounds such as endotoxins from the lumen to the lamina propria (Rohr et al., 2020). In contrast, consumption of high-fat/high-sugar diets affects the integrity of the intestinal barrier as well as the microbiota composition and functionality (dysbiosis). LPS is a major component of the outer membrane from both commensal and pathogenic gram-negative bacteria, and it plays a key role in host-pathogen interactions with the immune system. Low concentrations of LPS in the blood are associated with good maintenance of the immune system (Gnauck et al., 2016); however, dietary patterns linked to dysbiosis translate into a greater passage of LPS from the intestinal lumen towards the lamina propria, and consequently, into the blood circulation. This phenomenon is known as metabolic endotoxemia. This condition is characterized by the activation of the immune system, thus inducing systemic inflammation by increasing pro-inflammatory secretion of Tumour Necrosis Factor alpha (TNF-α) and Interleukin-6 (IL-6), especially in tissues involved in the metabolism of sugars and lipids, such as the liver and adipose tissue (Rohr et al., 2020). This situation contributes to the development of metabolic diseases, including type 2 diabetes, atherosclerosis and cardiovascular disease (Gnauck et al., 2016; Hersoug et al., 2016).

The precise pathway by which LPS is transported through the gut barrier remains controversial. However, currently, different mechanisms for LPS transport across the intestinal barrier have been proposed: (1) paracellular transport by passive diffusion associated with an increase in gut permeability due to tight junction alterations (Gil-Cardoso et al., 2017); (2) a transcellular pathway through cell-associated antigen passage as intestinal-epithelial microfold cells or goblet cells that are implicated in transporting antigens from the intestinal lumen to immune cells (Ghoshal et al., 2009); (3) receptor mediated endocytosis through clathrin- or caveolin-dependent transcytosis in enterocytes and

* Corresponding author.
E-mail address: raul.beltran@urv.cat (R. Beltrán-Debón).

https://doi.org/10.1016/j.jff.2023.105566
Received 24 January 2023; Received in revised form 21 March 2023; Accepted 27 April 2023
Available online 6 May 2023

colonocytes (Guerville & Boudry, 2016); or (4) the chylomicron-associated pathway in which LPS is transported in newly released chylomicrons (CM) during the post-prandial period (Ghoshal et al., 2009; Hersoug et al., 2016). Indeed, intestinal epithelium cells of the proximal intestine express the Cluster of Differentiation 36 (*CD36* or *Cd36* for human and rat, respectively) and Scavenger Receptor Class B type 1 (*SRB1* or *Srb1* for human and rat, respectively). These are both involved in endocytosis and CM-associated pathways by uptaking fatty acids, triglycerides and other dietary lipids (Hersoug et al., 2016). They act as sensors of dietary lipids, thus leading to an optimization of the size of CM produced during the postprandial stage (Ghoshal et al., 2009).

Traditional approaches to deal with obesity and its related metabolic endotoxemia were based on weight loss through eating a healthy diet and practising sport. In recent years, new anti-obesity treatments based on nutrition supplementation have been studied. Bioactive compounds, particularly flavonoids, are chemical components found in small quantities in food and have demonstrated beneficial effects on inflammatory pathways, barrier integrity and microbiota composition (Gil-Cardoso et al., 2016). The most abundant flavonoids in the Western diet are proanthocyanindins (PAC), also known as condensed tannins (Bladé et al., 2016). PAC are oligomers and polymers of monomeric flavan-3-ols mainly found in foods and beverages of vegetal origin that are ingested daily, such as grapes, cocoa, chocolate, red wine and green tea (Bladé et al., 2016; Salvadó et al., 2015; Smeriglio et al., 2017). PAC have been attributed to a wide range of biological activities as they modulate pathways involved in chronic inflammation, lipid homeostasis, energy metabolism, apoptosis and cell cycle arrest (Bladé et al., 2016). In relation to their function in lipid metabolism, PAC repress lipoprotein secretion, inhibit the absorption of dietary lipids and reduce CM secretion by enterocytes (Moreno et al., 2003; Quesada et al., 2012). Therefore, PAC have been attributed hypotrigliceridemic and hypolimidemic effects (Moreno et al., 2003; Quesada et al., 2012).

In previous studies, we demonstrated that PAC are involved in maintaining the intestinal barrier (González-Quilen et al., 2020) and reducing metabolic endotoxemia acting on the paracellular pathway in CAF-fed rats (Gil-Cardoso et al., 2018). Now, with the aim of obtaining a more holistic view of the effects and mechanisms of GSPE for modulating LPS transport, we have studied the receptor-mediated endocytosis and CM-associated pathways. In this study, PAC are evaluated as possible modulators of LPS translocation through the intestinal barrier using both *in vitro* and *in vivo* models of intestinal dysfunction.

2. Materials and methods

2.1. Proanthocyanidin extract

The grape-seed extract enriched in proanthocyanidins (GSPE) was provided by *Les Dérivés Résiniques et Terpéniques* (Dax, France). According to the manufacturer, the GSPE composition used in this study contains monomers (21.3%), dimers (17.4%), trimers (16.3%), tetramers (13.3%) and oligomers (5–13 units; 31.7%) of flavan-3-ols. A more detailed analysis of GSPE composition is shown in Table 1.

2.2. Chemicals

Dulbecco's Modified Eagle's Medium (DMEM) with 4.5 g/ml glucose, glutamine, 0.5 g/L trypsin-versene mixture solution and penicillin–streptomycin were purchased from Lonza Bioscience (Switzerland). HEPES buffer, Fetal Bovine Serum (FBS), fungizone, lipopolyssacharide (LPS) from *Escherichia coli O111:B*, oleic acid, sodium taurocholate, egg lecithin and phosphate buffer saline (PBS) were all purchased from Sigma Aldrich (Madrid, Spain). Sodic pentobarbital was purchased from Fagron Iberica (Barcelona, Spain). Heparin was provided by Deltalab (Barcelona, Spain). Total RNA was isolated from frozen intestinal segments using Trizol reagent (Ambion, MA, USA) according to the manufacturer's protocol.

Table 1
Main phenolic compounds of the GSPE used in this study, analysed by HPLC-MS/MS.

Compound	Concentration (mg/g)
Gallic acid	31.07 ± 0.08
Protocatechuic acid	1.34 ± 0.02
Vanillic acid	0.77 ± 0.04
PA dimer B2	33.24 ± 1.39
PA dimer B1[1]	88.80 ± 3.46
PA dimer B3[1]	46.09 ± 2.07
Catechin	121.32 ± 3.41
Epicatechin	93.44 ± 4.27
Dimer gallate	8.86 ± 0.14
Epicatechin gallate	21.24 ± 1.08
Epigallocatechin[2]	0.03 ± 0.00
PA trimer[1]	4.90 ± 0.47
PA tetramer[1]	0.05 ± 0.01

Extracted from (Margalef et al., 2016). The results are expressed on a wet basis as the means ± SD (n = 3) in mg of phenolic compound/g of GSPE. Abbreviations: *GSPE: Grape seed proanthocyanidin extract; PA: proanthocyanidins.* [1]Quantified using the calibration curve for proanthocyanidin B2. [2]Quantified using the calibration curve for epigallocatechin gallate.

2.3. Lipid mixture and GSPE solution preparation

Fatty acid micelles were prepared according to the adapted method used by *Yao et al.* (Yao et al., 2013). A 10X lipid mixture (LM) was prepared by mixing oleic acid, sodium taurocholate and egg lecithin (OA:NaTC:LC = 20 mM:10 mM:13.6 mM) in PBS 1X. To ensure complete homogenization, the solution was maintained in agitation overnight at room temperature and then sterilized by filtration with a syringe coupled to a 22 μm pore-size filter. 10X LM stock solution was stored at −20 °C prior to use.

GSPE was frozen upon receipt at −80 °C until the treatment day and kept in darkness. On the day of the assay, the GSPE solution was prepared freshly in 10% ethanol in pyrogen-free water.

2.4. Cell culture

Human epithelial colorectal adenocarcinoma Caco-2 cells were purchased from the European Collection of Authenticated Cell Cultures (ECACC). Cells were cultured and maintained in an incubator at 37 °C and 5% CO_2 in DMEM 4.5 g/ml glucose supplemented, 0.02 mM glutamine, 1 U/mL-1 μg/ml penicillin/streptomycin solution, 0.1 mM HEPES, 0.1% FBS and 0.01% fungizone. Cells were split at a 1:4 ratio when they reached 70–80% confluence using 0.5 g/L trypsin-versene mixture solution. The medium was changed every two–three days.

Cells were differentiated for 21 days using transwell inserts (Millicell, Northeim, Germany) in 6-well and 12-well plates (Greiner Bio-one, Madrid, Spain) to imitate the thin epithelial-cell monolayer. In 6-well plates, 200,000 cells/2 ml were seeded at the upper part of the insert of each well and, 65,000 cells/0.4 ml were seeded in the 12-well plates. Basolateral medium contained 1 ml and 2.5 ml of supplemented DMEM for 12-well and 6-well plates, respectively.

2.5. In vitro chylomicron production

The experimental procedure to induce *in vitro* chylomicron production was adapted from *Yao et al.* (Yao et al., 2013). Colourless medium was used for colorimetric determinations. The experimental medium was the same cell culture medium described in 2.4; however, it was not supplemented with FBS to avoid possible interferences of triglycerides contained in it.

Firstly, 10X LM stock solution prepared previously was thawed and diluted with experimental medium. After the cells were washed with PBS 1X, the different study treatments were added: (1) Control

containing experimental medium; (2) LPS (1 μg/ml); (3) LM; (4) LM+LPS; (5) LPS+GSPE (250 μg/ml); (6) LM+GSPE; and (7) LM+LPS+GSPE. After four hours of incubation, apical and basolateral media were collected and stored at −80 °C until analysis.

2.6. Lipoprotein fractionation

NaCl density gradient ultracentrifugation was used to isolate the CM-rich fraction from other types of lipoproteins. The procedure was adapted from *Nauli et al.* (Nauli et al., 2014). Basolateral media from 6-well plates were mixed with the corresponding amount of NaCl to obtain a solution with a density of 1.006 g/ml. This density mixture was then carefully overlaid with 500 μl of pyrogen-free water and subjected to ultracentrifugation (16,000 rpm, 30 min, 4 °C; Beckman Coulter, JA-25.15 rotor). The top 500 μl was carefully isolated to obtain a CM enriched fraction. Samples were stored in pyrogen-free tubes at −80 °C prior to determinations.

2.7. Animal models

Female Wistar rats (240–270 g) were purchased from Charles River Laboratories (Barcelona, Spain). After one week of adaptation, the rats were individually caged in animal quarters at 22 °C with a 12 h light/12 h dark cycle and were fed *ad libitum* with a standard chow diet (Panlab 04, Barcelona, Spain) and tap water. After the acclimation period, rats were randomly distributed into four experimental groups (n = 7–10/group). The control group (STD) was fed only with a standard chow diet. In addition to the chow diet, the other three groups received a cafeteria (CAF) diet as a model of a high-fat/high-sucrose diet (CAF groups). Two CAF groups were also supplemented with an oral dose of 500 mg GSPE/kg body weight at different times. The preventive treatment group (PRE) was administered GSPE during 10 days before the CAF diet challenge, whereas the simultaneous intermittent treatment-CAF (SIT) group received GSPE together with the cafeteria diet every other week (Fig. 1).

The CAF diet consisted of bacon, sausages, biscuits with pâté, carrots, muffins and sugared milk to induce voluntary hyperphagia (Sampey et al., 2011). This diet was offered freshly every day to the animals for 17 weeks, which was the entire duration of the study. The energy content of each diet has been described previously by *Ginés et al.* (Ginés et al., 2018).

GSPE was dissolved in tap water and was administered orally by gavage to the rats at 18:00 h for each treatment in a volume of 500 μl, one hour after removing all available food. Non-supplemented animals received tap water as a vehicle.

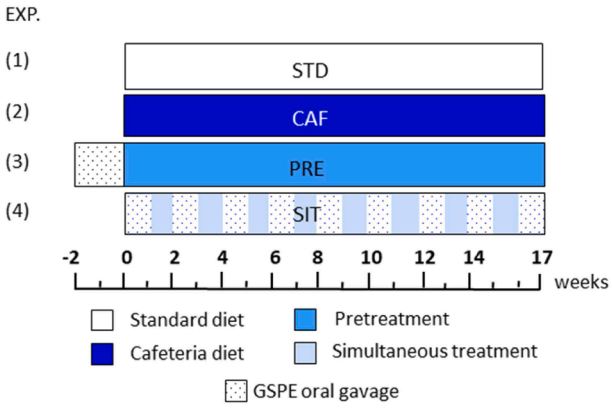

Fig. 1. Schematic diagram of the experimental design. All animals were subjected to adaptation to the environment and to oral gavage during one week before the onset of the experiment. **(1) STD:** rats receiving the standard diet during the whole experiment; **(2) CAF:** rats receiving the standard diet before the cafeteria diet intervention; **(3) PRE:** rats receiving a preventive treatment with GSPE for 10 days before the cafeteria diet challenge; **(4) SIT:** rats receiving GSPE treatment simultaneously and intermittently with the cafeteria diet every other week. Abbreviations: *CAF, cafeteria diet; GSPE, Grape Seed Proanthocyanidin Extract; STD, Standard diet.*

All procedures involving the care and use of animals in this work were reviewed and approved by The Animal Ethics Committee of the Universitat Rovira i Virgili (code: 0152S/4655/2015).

2.8. Blood and tissue collection

At the end of the study, animals were fasted for 4 h, anesthetized with sodic pentobarbital (70 mg/kg body weight) and exsanguinated from the abdominal aorta. The blood was collected using heparin (Deltalab, Barcelona, Spain) as an anticoagulant. Plasma was obtained by centrifugation (1500×g, 15 min, 4 °C) and stored at −80 °C until analysis. Mesenteric adipose tissue (MWAT), liver, and gut sections were rapidly removed, weighed and frozen in liquid nitrogen before storage at −80 °C until analysis.

2.9. Morphometric and biochemical parameters

LPS, triglycerides (TAG) and insulin concentration in plasma, and the HOMA-IR index were determined as previously described (Gil-Cardoso et al., 2018; Ginés et al., 2018). LPS levels in cell culture media, liver and MWAT homogenates were measured using the ToxinSensor™ Chromogenic LAL Endotoxin Assay Kit (GenScript, Spain). A colorimetric enzyme commercial kit was used to measure the TAG concentration (QCA, Amposta, Spain). The apolipoprotein B48 (APOB-48) concentration in basolateral media was quantified using a commercial ELISA kit (MyBiosource, Brussels, Belgium).

2.10. Quantitative real-time PCR

Total mRNA was isolated from 50 mg of duodenum, ileum and colon using Trizol Reagent (Thermo Fisher Scientific, Waltham, MA, USA) following the manufacturer's instructions. RNA from Caco-2 cells was extracted using an RNeasy Mini kit (Qiagen, Hilden, Germany). cDNA was obtained by reverse transcription of total RNA using the High Capacity cDNA Reverse Transcription kit (Applied Biosystems, Madrid, Spain) following the manufacturer's instructions. Quantitative real-time polymerase chain reaction (qPCR) was carried out in the Bio-Rad CFX96 Real-time PCR Systems (Bio-Rad Laboratories, Barcelona, Spain). All samples were run in duplicate in 96-well reaction plates.

The gene expression of *SRB1/Srb1* and *CD36/Cd36* were measured in both *in vitro* and *in vivo* experiments. Cannabinoid receptor 1 gene expression (*Cnr1*) was also determined in rat colon samples. For rat samples, the iTaq Universal SYBR® Green Supermix (Bio-Rad) was used, together with the respective forward and reverse primers (Biomers, Germany) for the targeted rat genes (Table 2). The results were normalized with respect to the mRNA levels of Hypoxanthine-guanine Phosphoribosyl Transferase (*HPRT or Hprt* for human and rat, respectively) and cyclophilin-E (*Ppia*) genes, used as housekeeping controls. The relative mRNA expression levels were calculated following the $2^{-\Delta\Delta Ct}$ method. The identity and purity of the amplified products were assessed by melting curve analysis.

For cell culture samples, we used the TaqMan Universal PCR Master Mix (Applied Biosystems), together with the respective specific TaqMan probes (Applied Biosystems): Hs00354519_m1 for *CD36*, Hs00969821_m1 for *SRB1* and Hs02800695_m1 for *HPRT*. The relative amount of mRNA was normalized to the *HPRT* as the endogenous control gene.

Reactions with the iTaq Universal SYBR® Green Supermix were performed using the following thermal profile: 30 s at 95 °C, 40 cycles of 5 s at 95 °C and 30 s at 60 °C. Reactions with the TaqMan Universal PCR Master Mix were performed as previously described by *Gil-Cardoso et al.* (Gil-Cardoso et al., 2018). The relative mRNA expression levels were calculated following the $2^{-\Delta\Delta Ct}$ method. Zoonulin-1 (*Zo-1*), Occludin-1

Table 2
Primer sequences used for Quantitative real-time PCR of rat tissues.

Gene	Genbank number	Forward primer (5′ – 3′)	Reverse primer (5′ – 3′)
Cd36	NM_031561.2	GTCCTGGCTGTGTTTGGA	GCTCAAAGATGGCTCCATTG
Srb1	NM_031541.2	AGCCCCACTTCTACAATGCT	TGGCTCGATCTTCCCTGTTT
Cnr1	NM_012784.5	TCGACAGGTACATATCCATTCACA	GAGAGGCAACACAGCGATTACTACT
Hprt	NM_012784.5	TCCCAGCGTCGTGATTAGTGA	CCTTCATGACATCTCGAGCAAG
Ppia	NM_017101.1	CCAAACACAAATGGTTCCCAGT	ATTCCTGGACCCTTTTCGCT

Abbreviations: *Cd36, Cluster of Differentiation 36; Cnr1, Cannabinoid receptor type 1; Hprt, Hypoxanthine-guanine phosphoribosyl transferase; Ppia, cyclophilin-E; Sr-b1, Scavenger receptor class B type 1.*

(*Ocln*), Claudin-1 (*Cldn1*) and Jam-A gene expression were previously determined by *Gil-Cardoso et al.* (Gil-Cardoso et al., 2018).

2.11. DNA methylation analysis

Genomic DNA was extracted from colon samples using a DNeasy Blood and Tissue Kit (Qiagen, Hilden, Germany). DNA was subjected to bisulfite modifications using a commercially available kit (Zymo Research, Irvine, CA, USA). After that, DNA methylation analysis was carried out by pyrosequencing. Primers for rat *Cnr1*, the gene coding for the cannabinoid receptor type 1 (CNR1), targeting eight CpG sites, were generated according to Pyro Mark Assay design Assay Software version 2.0 (Qiagen). Bisulfite-treated DNA was amplified using a PyroMark PCR kit (Qiagen) according to the manufacture's protocol. The PCR protocol was as follows: 95 °C for 15 min, followed by 45 cycles of 94 °C for 30 s, 56 °C for 30 s, 72 °C for 30 s, and finally, 72 °C for 10 min. PCR products were checked in an agarose electrophoresis. PyroMark Q24 (Qiagen, Hilden, Germany) was used to perform pyrosequencing methylation analysis and the PyroMark Q24 ID version 1.0.9 software (Qiagen) was used to calculate the methylation level. This software calculates the methylation percentage mC/(mC + C) (where mC is methylated cytosine and C is unmethylated cytosine) for each CpG site and makes quantitative comparisons possible. Quantitative methylation results were expressed both as a percentage of individual CpG sites and as an average of the methylation percentage of all the investigated CpG sites. Table 3 shows the primer sets for the *Cnr1* pyrosequencing analysis.

2.12. Short chain fatty acid quantification

Short chain fatty acids (SCFAs) (propionic, isobutiric, butyric, isovaleric, and valeric) concentrations were determined in cecal content thawed at 4 °C. The experimental procedure was performed according to *Ginés et al.* (Ginés et al., 2019).

2.13. Statistical analysis

The results are expressed as the mean value ± the standard error of the mean (SEM). For *in vitro* experiments, statistical comparisons between groups were assessed by a two-sided Student's *t*-test. For *in vivo* experiments, non-parametric Kruskal-Wallis and Mann-Whitney tests were used. Pearson's correlation coefficient was evaluated to assess relationships between different parameters. A multiple linear regression analysis with backward variable selection was carried out to identify independent predictors of LPS circulating levels. Variables included in the model were ovalbumin (OVA) and TAG plasma levels, butyric acid in cecal content, and *Cldn-1*, *Cd36* and *Cnr1* gene expression in different gut sections. These variables presented strong correlation coefficients with LPS levels. We considered p-values < 0.05 as statistically significant. Analyses were performed with XLStat 2021.03.1 (Addinsoft, Barcelona, Spain).

Table 3
Primer sets used for pyrosequencing.

Rat	*Cnr1*	Forward	5′ – AGAAGGGTAAGATTTGGTATAGTG – 3′
		Biot-Reverse	5′ – AACTATACAACTAAATAAACACCACATTA – 3′
		Sequencing	5′ – GTGGAGTTTGGGAATAGTTT – 3′

3. Results

3.1. GSPE as a modulator of LPS transport across the intestinal barrier

Our group obtained previous results (Ginés et al., 2018) that demonstrated that consuming a CAF diet significantly increased the body weight in the CAF-fed rats compared to the chow diet-fed rats (346.2 ± 12 vs 273.7 ± 7.8). Interestingly, the simultaneous GSPE treatment was effective in reducing body weight from the second week until the end of the experiment (297.3 ± 9.8 vs 346.2 ± 12). Moreover, in the SIT groups, visceral adiposity (8.4 ± 0.6 vs 11.8 ± 0.8) and brown adipose tissue (0.8 ± 0.1 vs 1.0 ± 0.1) were significantly reduced compared to CAF group. Furthermore, CAF diet significantly induced an increase in LPS circulating levels in rats. We also found that a pharmacological dose of GSPE (500 mg/kg body weight) was able to reduce metabolic endotoxemia in both PRE and SIT groups (Gil-Cardoso et al., 2018). The details of the experimental groups are shown in Fig. 1.

In order to study how GSPE modulates LPS transport, we first explored the associations between metabolic endotoxemia and variables related to barrier integrity and intestinal permeability. We found that the LPS concentration was negatively associated with the transepithelial electrical resistance (TEER) values in duodenum and with *Cldn1* gene expression in ileum (Fig. 2A and F, respectively) showing a relationship between metabolic endotoxemia and the paracellular pathway. Furthermore, the LPS concentration was strongly positively associated with the TAG concentration in plasma (Fig. 2B), suggesting a lipoprotein-associated LPS transport. Finally, the fact that LPS and OVA levels in plasma were positively associated (Fig. 2D), led us to investigate receptor mediated endocytosis because this is one of the mechanisms of OVA transport across the intestinal barrier.

3.2. GSPE modulation of CM-associated LPS transport

To study the potential modulation of GSPE on CM-associated LPS transport, Caco-2 cell CM-production was induced using lipids. We first quantified TAG levels in the CM-rich fraction. As observed in Fig. 3A, we were able to induce *in vitro* CM production up to 3-fold with respect to the control cells, although the differences were not statistically significant. GSPE supplementation seemed to reduce TAG levels ($p > 0.05$).

Moreover, the LPS levels were also quantified in CM-rich fraction media to assess the amount of LPS that crosses the cell monolayer associated with CMs and the potential effect of GSPE-supplementation. The LPS levels were significantly higher in LPS-treated cells compared with the control (Fig. 3B). Interestingly, when administered together with lipids, the LPS levels were slightly higher than LPS administration alone. This suggests an increase in LPS transport associated with CMs. GSPE decreased CM-associated LPS levels in the co-culture of LM+LPS but not when cells were cultured with LPS alone (Fig. 3B).

Considering these results, we wondered if GSPE was modulating LPS transport by reducing CM production. For this reason, we measured the

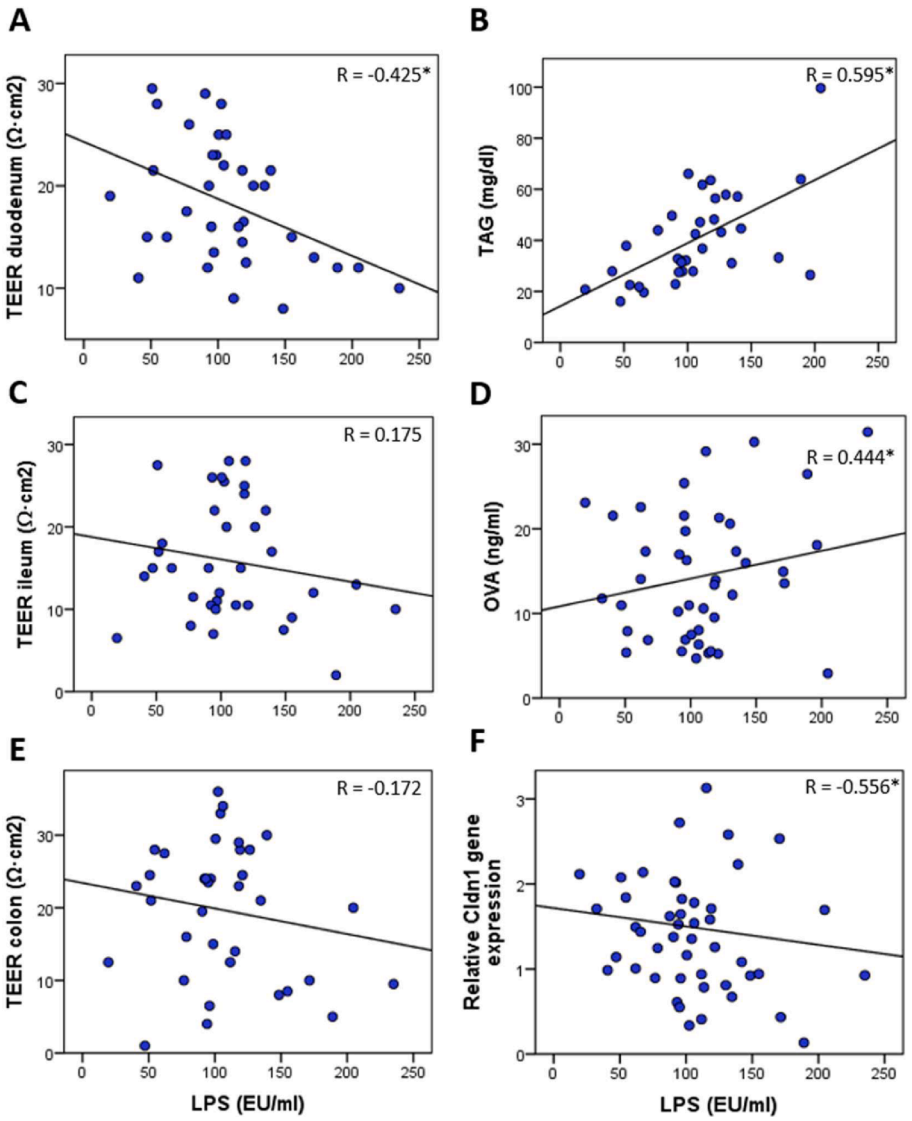

Fig. 2. Pearson's correlations between LPS levels in plasma and different parameters: **(A, C, E)** Transepithelial Electrical Resistance (TEER); **(B)** Plasma triglycerides (TAG); **(D)** Ovalbumin (OVA); **(F)** Claudin-1 (*Cldn1*) relative gene expression in the ileum; $n = 35–54$; $^{*}p < 0.05$.

APOB-48 levels in the cell culture media. The APOB-48 levels were increased up to 4-fold in all treatments containing LM in c1omparison with the control and non-stimulated cells, thus confirming CM secretion in our *in vitro* model. However, GSPE did not modify the APOB-48 levels (Fig. 3C), which indicates that GSPE was not reducing LPS transport by decreasing CM synthesis. To assess whether GSPE induces a reduction in CM size, we calculated the TAG/APOB-48 ratio. As shown in Fig. 3D, although not significant, GSPE limited CM size when treated with LM.

3.3. GSPE modulation of LPS transport through receptor-mediated endocytosis

We studied the receptor-mediated endocytosis pathway by evaluating *CD36* and *SRB1* gene expression in Caco-2 cells. LPS treatment induced a significant increase in *CD36* expression. Moreover, when cells were treated with a mixture of LM+LPS, the mRNA levels were even higher compared to individual treatments. GSPE induced a significant decrease in *CD36* expression compared to the respective controls (Fig. 3E). With respect to *SRB1*, LM treatment increased its expression levels compared to the control. Similar to the results observed for *CD36*, the combination of LM+LPS induced a higher increase in *SRB1* expression. Contrary to *CD36*, GSPE increased *SRB1* mRNA levels when administered together with LM and with the co-culture with LM+LPS (Fig. 3F).

To validate these *in vitro* results, we measured *Cd36* and *Srb1* gene expression in the duodenum, ileum and colon of obese rats. In duodenum, although changes were not significant, *Cd36* expression was higher in the PRE group compared to the CAF group (Fig. 4A) and *Srb1* did not show any difference between treatments (Fig. 4B). In the ileum, CAF-fed rats showed an increase in *Cd36* mRNA levels with respect to the control, and the simultaneous treatment with GSPE tended to reduce mRNA levels (Fig. 4C). In contrast, the CAF diet seemed to induce a reduction in *Srb1* mRNA levels compared with the control, and GSPE had no effect on gene expression (Fig. 4D). No changes in gene expression were observed in the colon (Fig. 4E-F).

3.4. GSPE modulates LPS accumulation in the liver

In previous animal studies, we showed that the CAF diet provoked metabolic endotoxemia (Gil-Cardoso et al., 2018). Moreover, it has been described that metabolic endotoxemia is directly associated with insulin resistance due to LPS tissue accumulation, especially in liver and white adipose tissue (Ghosh et al., 2020). To assess LPS accumulation, we measured LPS levels in liver and MWAT homogenates. In the liver, the

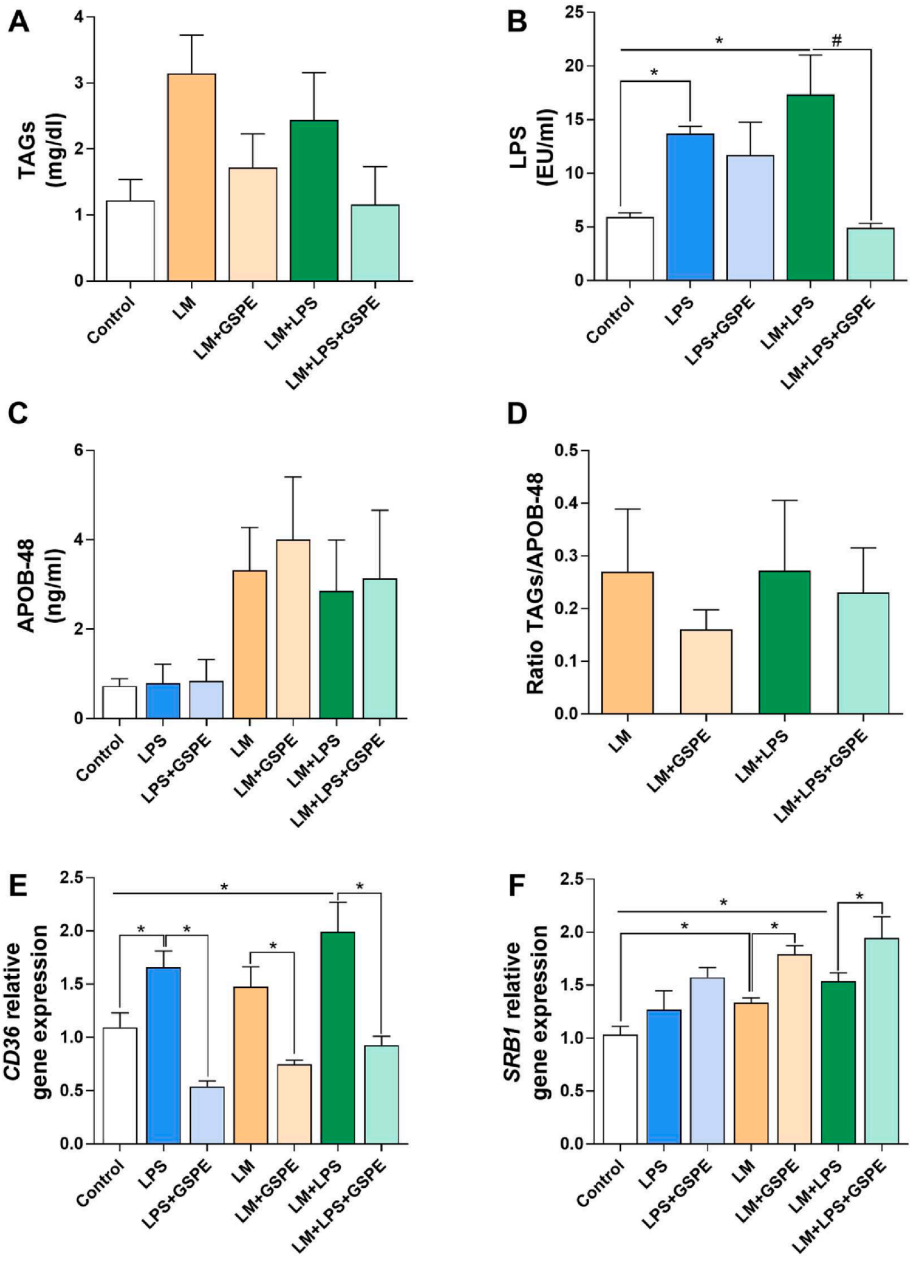

Fig. 3. Caco-2 cells as an *in vitro* model for LPS intestinal translocation associated with CMs**.** Cells were stimulated with either LPS (1 μg/ml), LM, or LM + LPS and also with or without GSPE (250 μg/ml). **(A-C)** TAG, LPS and APOB-48 levels in the CM-rich fraction, respectively; **(D)** TAG/APOB48 ratio; **(E-F)** CD36 and SRB1 gene expression levels, respectively. Abbreviations: *APOB-48, Apolipoprotein B48; CD36, Cluster of Differentiation 36; GSPE, Grape Seed Proanthocyanidin Extract; LM, Lipid mixture; LPS, lipopolysaccharide; TAG, triglycerides; SRB1, Scavenger Receptor Class B member 1.* Values are means ± SEM (n = 2–9). *p < 0.05. #Trends: 0.05 < p-value < 0.1.

CAF diet induced a higher accumulation of LPS compared to the control animals. GSPE significantly decreases LPS accumulation in the liver when administered both preventively and simultaneously with the CAF diet and was statistically different in the SIT group (Fig. 5A). No changes were observed in the LPS levels in adipose tissue (Fig. 5B).

3.5. GSPE epigenetic modulation of the endocannabinoid system

Given our results, in which intestinal permeability is affected by the CAF diet, and GSPE supplementation seems to have a modulatory effect, we aimed to determine its mechanism of action. One potential mechanism is the modulation of the endocannabinoid system (ECS). CNR1 activation regulates intestinal permeability and inflammation (Chen et al., 2020), especially in a context of obesity (Pucci et al., 2021). For this reason, we studied whether GSPE could be modulating intestinal permeability and LPS translocation at this level in our diet-induced obesity animal model.

We evaluated *Cnr1* gene expression in the colon because it is the most abundant LPS-containing intestinal segment due to the presence of microbiota. The CAF diet induced an increase in *Cnr1* mRNA levels compared with the STD group. Moreover, GSPE simultaneous supplementation reduced *Cnr1* expression (Fig. 6A).

To further study the possible mechanism of GSPE modulation on *Cnr1* expression in the colon, we performed an epigenetic analysis of the *Cnr1* promoter's CpG site methylation (Fig. 6B). Although no changes in the average methylation were observed (Fig. 6C), the methylation of the promoter in position 7 was higher in the SIT group than in the CAF group (Fig. 6D). This result could partially explain the decrease in *Cnr1* gene expression (Fig. 6A). Furthermore, preventive supplementation with GSPE also reduced the DNA methylation pattern of the *Cnr1* promoter with respect to the CAF rats in positions 4 and 6 (Fig. 6D).

3.6. Gut microbiota as a modulator of the endocannabinoid system

Gut microbiota and SCFAs can be altered by the consumption of sugars and saturated fats (Rohr et al., 2020). Moreover, gut microbiota

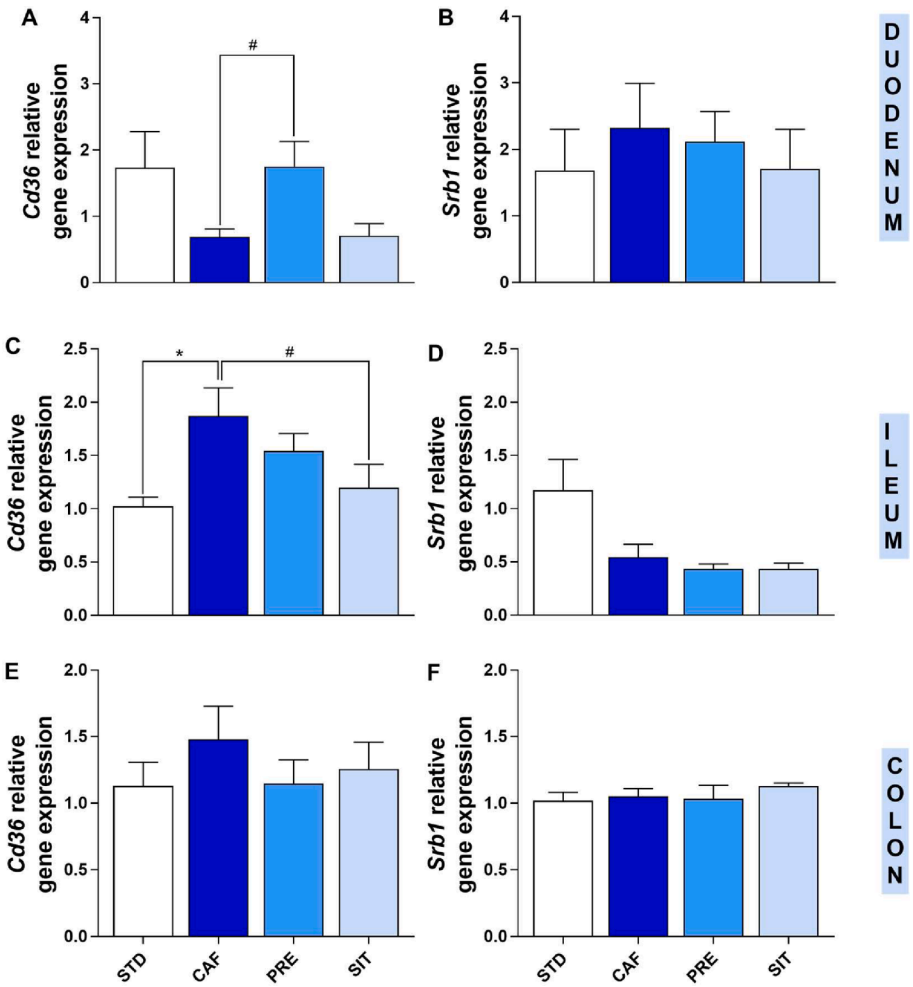

Fig. 4. The effect of GSPE treatment on CD36 and SRB1 gene expression in the intestine of diet-induced obese rats. **(A-B)** Gene expression in the duodenum; **(C-D)** Gene expression in the ileum; **(E-F)** Gene expression in the colon. The expression of target genes was normalized to Hprt. Abbreviations: *Cd36, Cluster of Differentiation 36; Srb1, Scavenger Receptor Class B member 1. Values are means ± SEM (n = 4–10). *p < 0.05. #Trends: 0.05 < p-value < 0.1.*

can modulate intestinal permeability and LPS translocation through the interaction with ECS (Chen et al., 2020; Muccioli et al., 2010). Therefore, we wanted to evaluate the possible correlations between some cecal SCFAs and the expression of *Cnr1* and the methylation pattern of its promoter (Table 4). The expression of *Cnr1* was negatively correlated with methylation levels in positions 2 and 5. We also found that positions 2 and 5 were positively correlated with the isobutyric acid levels, and position 8 with isovaleric acid. Moreover, we also found some negative correlations between positions 2, 3, 4, 6, and 7 with valeric acid in the cecal content (Table 4). In addition, the methylation of positions 2, 3, 4 and 5 were negatively associated with insulin resistance indexes such as HOMA-IR and insulin levels (Table 4).

3.7. Gut microbiota SCFAs are associated with intestinal permeability

With this established correlation between the *Cnr1* methylation pattern and SCFAs, we aimed to evaluate the possible associations between SCFAs and intestinal permeability, LPS transport and tissue accumulation (Table 5). *Srb1* expression levels were negatively correlated with propionic acid and positively with butyric acid. Interestingly, accumulation of TAG in the liver, plasma LPS and *Cd36* gene expression in the colon were positively associated with isobutyric acid levels. Moreover, butyric acid was negatively correlated with plasma OVA levels and positively with *Srb1* gene expression in the colon. Valeric acid was positively associated with the accumulation of LPS in the MWAT (Table 5).

3.8. Paracellular pathway, receptor-mediated endocytosis and gut microbiota as major contributing factors of increased metabolic endotoxemia

With this scenario, we decided to generate a multiple regression model to explain the major factors studied that contribute to intestinal LPS translocation and subsequent metabolic endotoxemia. The independent variables were OVA and TAG levels in plasma, *Cldn1*, *Cd36* and *Cnr1* intestinal gene expression, and butyric acid cecal concentration. Applying the backward exclusion method, we obtained a reduced model to explain LPS accumulation in plasma through OVA levels, *Cd36* gene expression in the ileum and butyric acid concentration. Hence, the most important factors determining LPS translocation are related to paracellular, receptor-mediated endocytosis and CM-associated pathways, as well as gut microbiota, with a corrected R^2 of 0.767 (Table 6).

4. Discussion

The excessive consumption of dietary sugars and fat causes intestinal barrier dysfunction, provoking metabolic endotoxemia and systemic inflammation. Furthermore, as stated by *Cani et al.*, metabolic endotoxemia triggers obesity, diabetes and other related metabolic disorders (Cani et al., 2007). New therapeutic approaches are needed to treat metabolic endotoxemia, and numerous studies have found that proanthocyanidins play an important role in protecting the intestinal barrier, especially through their anti-inflammatory activity. This study aims to

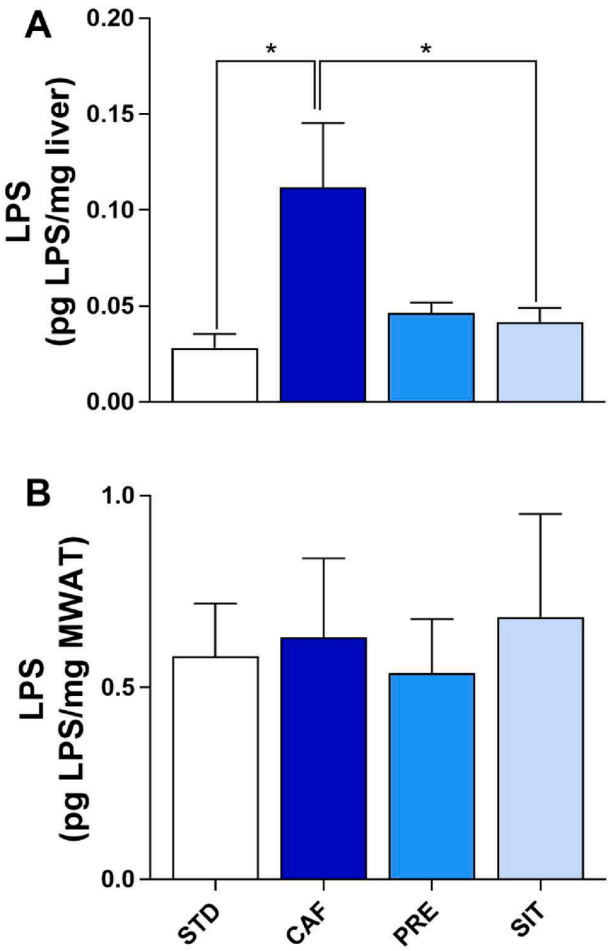

Fig. 5. GSPE decreases LPS accumulation in the liver. LPS quantification in **(A)** liver and **(B)** MWAT homogenates. Abbreviations: *LPS, lipopolysaccharide; MWAT, mesenteric adipose tissue. Values are means ± SEM (n = 3–9). *p < 0.05.*

use both *in vitro* and *in vivo* experimental approaches to elucidate how GSPE could modulate intestinal LPS translocation not only through the paracellular pathway but also by receptor-mediated endocytosis and chylomicron-associated transport in a context of obesity.

Our group obtained previous results that demonstrated that a dose of 500 mg GSPE/kg body weight was capable of reducing the plasma levels of both LPS and OVA, as well as ameliorating intestinal damage in the duodenum and ileum caused by consuming a CAF diet (Gil-Cardoso et al., 2018). Now, we have found that LPS levels are associated with TAG in plasma in our *in vivo* model for diet-induced obesity, in agreement with results obtained in obese humans and high fat diet (HFD) fed mice (Clemente-Postigo et al., 2019; Kan et al., 2019). This association reinforced the idea that LPS is being transported associated with CM. Moreover, we also found that LPS and OVA circulating levels were positively correlated, suggesting that they might be transported by similar pathways across the intestinal barrier, such as receptor-mediated endocytosis and paracellular pathways (Yokooji et al., 2014). In fact, the paracellular pathway has already been described as a relevant mechanism for LPS translocation in the small intestine (Kim et al., 2012; Stephens & von der Weid, 2020). In agreement with this, we found that ileal *Cldn1* gene expression and TEER values in the duodenum were negatively correlated with LPS plasma levels. Regardless of the mechanism responsible for LPS translocation, any dietary intervention able to modulate the LPS transport across the intestinal barrier, and thus reduce the metabolic endotoxemia, would be of great interest.

Postprandial lipemia dysregulation is an important factor for cardiovascular diseases. Regarding LPS transport associated with CM, we observed that GSPE seems to reduce LPS passage *in vitro*. Several studies have demonstrated the protective effect of GSPE as it reduces hyperlipidemia (Ginés et al., 2018) and metabolic endotoxemia in CAF-fed animal models (Gil-Cardoso et al., 2018; González-Quilen et al., 2019). Our results also support the findings of *Quesada et al.*, who reported that a dose of 250 mg GSPE/kg body weight reduced TAG levels associated with CM in male rats fed with a chow diet after lard oil administration (Quesada et al., 2012). The GSPE hypotriacylglycerolaemic effect has been widely demonstrated (Downing et al., 2015; Pons et al., 2014; Quesada et al., 2009; Shi et al., 2019); however, whether the lipoprotein amount or size was modified, has not yet been elucidated. Although our results are not conclusive, they suggest that GSPE reduces TAG transport by reducing CM size, as APOB-48 levels were not affected by GSPE treatment. Taking all these results into account, we can hypothesize that GSPE might be modulating LPS transport associated with CM in an indirect way by reducing CM size. *Hayashi et al.* demonstrated that consuming a HFD had no effect on increasing CM production but it did affect the size in rats (Hayashi et al., 1990). *Yaman et al.* recently found that humans with a high postprandial TAG response

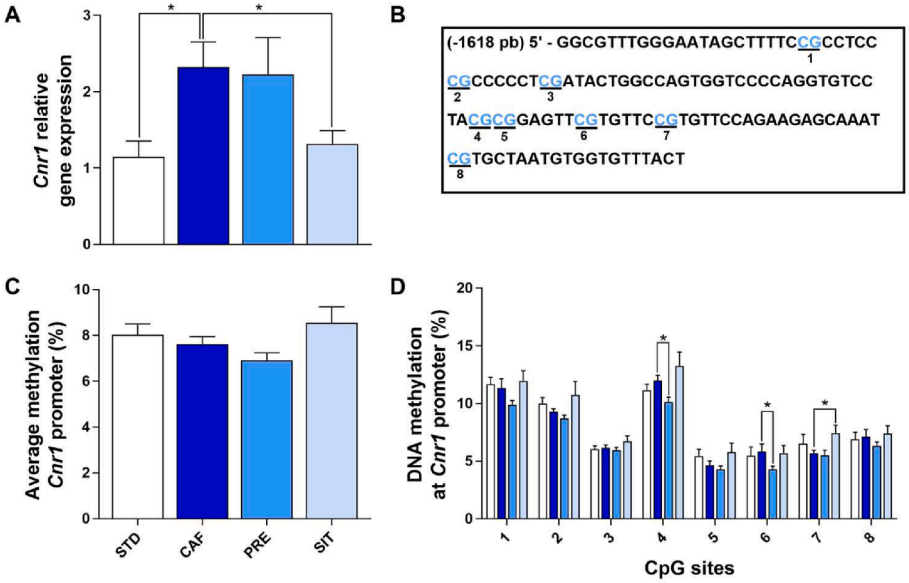

Fig. 6. Simultaneous treatment with GSPE modulates CNR1 expression, possibly through epigenetic mechanisms. **(A)** *Cnr1* gene expression; **(B)** Localization of the CpG sites (numbered from 1 to 8) of the *Cnr1* promoter; **(C)** Average DNA methylation from the CpG sites of a region of *Cnr1* promoter; **(D)** DNA methylation on 8 CpG sites of a region of the *Cnr1* promoter. The expression of target genes was normalized to *Ppia*. Abbreviations: *Cnr1, Cannabinoid receptor type 1. Values are means ± SEM (n = 3–9). *p < 0.05.*

Table 4
Correlation coefficients of cannabinoid receptor 1 gene expression and methylation values compared with cecal microbiota derived SCFAs and markers of intestinal permeability and insulin resistance.

Variables	Isobutyric	Butyric	Isovaleric	Valeric	Insulin	HOMA-IR	OVA	LPS	Colon Cnr1 gene expression
Colon Cnr1 gene expression	0.263	−0.225	0.198	0.283	0.266	**0.428***	**0.496***	0.132	
Cnr1 promoter methylation									
Position 1	0.088	0.101	−0.278	−0.095	−0.218	−0.306	−0.061	0.224	−0.382
Position 2	−0.009	−0.041	**0.524***	**−0.427***	**−0.623***	**−0.734***	−0.078	0.168	**−0.403***
Position 3	0.344	−0.249	0.295	**−0.481***	**−0.469***	**−0.542***	−0.177	0.100	−0.240
Position 4	0.260	−0.234	0.137	**−0.505***	**−0.465***	**−0.517***	0.070	0.215	−0.261
Position 5	−0.023	0.110	0.039	−0.284	**−0.424***	−0.378	−0.281	0.025	**−0.481***
Position 6	**0.573***	−0.207	−0.092	**−0.435***	−0.306	−0.333	−0.059	0.214	−0.047
Position 7	0.035	−0.117	0.137	**−0.569***	−0.428	−0.426	−0.312	−0.022	−0.410
Position 8	**0.439***	−0.202	0.042	−0.412	−0.403	−0.363	0.031	0.058	−0.142

Abbreviations: *Cnr1, Cannabinoid receptor type 1; LPS, lipopolysaccharide; OVA, ovalbumin;* n = 31–54; *p-values < 0.05.

Table 5
Correlation coefficients of short chain fatty acids with intestinal permeability and systemic inflammation markers.

Variables	Propionic	Isobutyric	Butyric	Isovaleric	Valeric
Plasma triglycerides (mg/dl)	−0.318	−0.224	0.032	−0.177	−0.276
Liver triglycerides (mmol/g tissue)	0.140	**0.485***	−0.144	−0.300	0.341
Plasma Ovalbumin (ng/ml)	0.279	0.354	**−0.459***	−0.033	0.068
Plasma LPS (EU/ml)	0.106	**0.445***	−0.169	0.104	−0.077
LPS in MWAT (pg/g tissue)	−0.156	−0.015	0.233	−0.184	**0.562***
Ileal gene expression					
Scavenger receptors					
Cd36	−0.099	**0.582***	−0.335	0.043	−0.245
Srb1	**−0.501***	−0.104	**0.608***	−0.050	0.050

Abbreviations: *Cd36, Cluster of Differentiation; LPS, lipopolysaccharide; MWAT, mesenteric adipose tissue; Srb1, Scavenger Receptor class B type 1*; n = 35–54; *p-values < 0.05.

Table 6
Multiple regression mathematical model to explain and predict metabolic endotoxemia and the relevance of intestinal permeability-related variables.

	Unstandardized coefficient	Typified coefficient	p-value
Model	**B (Confidence interval of 95%)**	**Beta**	
1			
OVA	10.018 (-38.494 – 58.530)	1.489	0.468
TAG	0.178 (-6.030 – 6.386)	0.074	0.913
Cldn1 gene expression	25.253 (-438.310 –	0.273	0.836
(ileum)	488.815)	1.171	0.372
Cd36 gene expression	95.312 (-263.955 –	−0.280	0.747
(ileum)	454.580)	1.205	0.456
Cnr1 gene expression	−12.718 (-160.805 –		
(colon)	135.368)		
Butyric	2.880 (-10.645 – 16.404)		
2			
OVA	10.989 (-10.027 – 32.004)	1.634	0.195
Cldn1 gene expression	30.580 (-226.776 –	0.331	0.730
(ileum)	287.936)	1.236	0.187
Cd36 gene expression	100.539 (-87.000 –	−0.330	0.574
(ileum)	288.077)	1.328	0.157
Cnr1 gene expression	−14.983 (-90.854 –		
(colon)	60.887)		
Butyric	3.172 (-2.203 – 8.546)		
3			
OVA	8.639 (3.142 – 14.136)	1.284	0.012*
Cd36 gene expression	80.514 (16.887 –	0.990	0.025*
(ileum)	144.141)	−0.156	0.525
Cnr1 gene expression	−7.085 (-35.373 –	1.119	0.046*
(colon)	21.203)		
Butyric	2.673 (0.080 – 5.265)		
4			
OVA	8.953 (4.261 – 13.645)	1.331	0.040*
Cd36 gene expression	87.653 (37.781 –	1.077	0.006*
(ileum)	137.526)	1.262	0.010*
Butyric	3.016 (1.086 – 4.945)		

Abbreviations: Cnr1, Cannabinoid receptor type 1; Cd36, Cluster of Differentiation; OVA, ovalbumin; TAG, triglycerides. *p-values < 0.05.

showed higher levels of TAG, APOB-48 and a bigger CM size (Yaman et al., 2021). Therefore, although our results need to be confirmed in future studies, this potential effect of GSPE might have an impact on both hypertriglyceridemia and metabolic endotoxemia management.

With respect to receptor-mediated endocytosis, the gene expression results were inconsistent between the *in vitro* and *in vivo* experiments. In the *in vitro experiment*, GSPE was able to reduce *CD36* gene expression. In animal models, the CAF diet increased *Cd36* expression in the ileum, and synchronic treatment with GSPE reduced it, as seen in the *in vitro* model. These results support that Caco-2 cells spontaneously change their morphological and functional features during the differentiation process, exhibiting a phenotype closer to small intestine enterocytes than colonocytes, as previously reported by different authors (Engle et al., 1998; Ferraretto et al., 2007; Sambuy et al., 2005). Moreover, as it has been described in the literature, *Cd36* is mainly expressed in the proximal small intestine (duodenum and jejunum), where lipid absorption and CM production take place (Pepino et al., 2014; Tran et al., 2011). Our results probably suggest that the non-absorption of fatty acids in the duodenum is being compensated in the ileum. Interestingly, the *SRB1* expression profile was the opposite to the *CD36 in vitro*. SRB1 is described as a multifactorial receptor, displaying positive and negative effects depending on the context. For example, upregulation of SRB1 expression constitutes a risk factor for obesity, whereas it plays a protective role in diabetes (Lenahan et al., 2019). In this study, GSPE increased *SRB1* gene expression *in vitro,* supporting previous results from experiments with obese rats treated with other antioxidants (Jeyakumar et al., 2007). We could also hypothesize that the increase in *SRB1* expression is a possible compensatory mechanism due to the reduction in *CD36* expression, and not related to the GSPE treatment.

Previous reports have shown that ECS controls the gut barrier function through a CNR1-dependent mechanism and obesity is characterized by ECS dysregulation (Pucci et al., 2019), leading to a higher intestinal permeability and metabolic endotoxemia (Chen et al., 2020; Muccioli et al., 2010). In our study, we found that the CAF diet increased *Cnr1* expression in the colon. Moreover, we demonstrated that GSPE modulates DNA methylation of the *Cnr1* promoter in the colon of CAF-fed rats. *D'Addario et al.* previously demonstrated *Cnr1* regulation by promoter methylation in animal models of anorexia nervosa (D'Addario et al., 2020) and obesity (Pucci et al., 2019). Moreover, the epigenetic regulator resveratrol modulates gut microbiota via interaction with ECS

in a HFD-induced obesity model (Chen et al., 2020). Taken together, our results suggest that GSPE might modulate intestinal permeability through epigenetic mechanisms at the ECS level. Moreover, the methylation profile of the *Cnr1* promoter was negatively associated with insulin and the HOMA-IR values. This supports previous results that positively correlated gut permeability with insulin resistance (Damms-Machado et al., 2017; Sidibeh et al., 2017).

We found interesting associations between SCFAs with intestinal permeability and metabolic endotoxemia-related parameters. SCFAs are products derived from bacterial fermentation of undigested carbohydrates, which play an important role in human health and metabolism (Silva et al., 2020). Butyric acid was negatively correlated with OVA plasma levels and positively with *Srb1* expression in the ileum. Our results support the idea that butyric acid is crucial in maintaining gut barrier integrity, especially avoiding LPS translocation through the paracellular pathway (Morrison & Preston, 2016). In contrast to the literature, we found that butyric acid did not have a protective effect against LPS-translocation via SRB1 (Tedelind et al., 2007; Venegas et al., 2019). Moreover, in contrast to butyric acid, the isobutyric levels were positively correlated with the TAG and LPS levels in plasma, as well as with the *Cd36* gene expression in the ileum. Then, increased isobutyric levels might be harmful for intestinal barrier integrity, promoting LPS translocation through both paracellular and receptor-mediated endocytosis pathways. In fact, high levels of isobutyric acid have been associated with negative effects in patients with cancer and metabolic syndrome (Ratajczak et al., 2021). Valeric acid was positively correlated with LPS levels in adipose tissue and negatively correlated with the *Cnr1* methylation pattern. In contrast to butyric acid, propionic acid was negatively associated with *Srb1* expression in the ileum, so that it exhibited a beneficial anti-inflammatory effect, as previously described (Tedelind et al., 2007; Venegas et al., 2019). Moreover, since dietary flavonoids are degraded by intestinal microbiota in the colon, the microbiota-derived metabolite profile depends on the flavonoids ingested. In accordance with our results, it has been previously demonstrated that GSPE decrease butyric acid levels in cecal content in both chow and CAF-diet fed animals (Casanova-Martí et al., 2018; Ginés et al., 2019). All things considered, since the microbiota is linked to intestinal homeostasis, we propose GSPE as an interesting and promising candidate for modulating dysbiosis and intestinal permeability.

In previously published research by our group, we found that our *in vivo* model for obesity showed a slight insulin resistance (Ginés et al., 2018). It has been described that gut permeability is directly associated with LPS tissue accumulation and insulin resistance, especially in liver and adipose tissue, where LPS exerts its cytotoxic activity (Ghosh et al., 2020). We found that LPS levels were five times higher in adipose tissue than in the liver. It has been described that the liver has mechanisms to detoxify LPS that are not present in adipose tissue (Cabral et al., 2021; Fox et al., 1990), such as the disposal of LPS through bile secretion, or enzymes in liver Kupffer cells that detoxify LPS (Guerville & Boudry, 2016). In our experimental animals, the CAF diet impaired these mechanisms, so that LPS levels increased in the liver; however, GSPE was able to restore this function. Interestingly, this lower LPS accumulation in the liver could be a sign of good hepatic functioning. In fact, in accordance with these results, we reported in previous studies that the SIT group had a reduced TAG accumulation in the liver compared to the CAF group. This supports that GSPE improves the hepatic function and reduces the risk of a low grade of inflammation and hepatic steatosis (Ginés et al., 2018). The proposed GSPE protective mechanisms against metabolic endotoxemia are shown in Fig. 7.

5. Conclusion

In conclusion, this is the first study that evaluates how GSPE can modulate metabolic endotoxemia considering several pathways, and which studies potential action mechanisms such as the modulation of gut microbiota and ECS. We suggest that *Cnr1* could be a major therapeutic target for treatment of metabolic endotoxemia, and GSPE could be used as a prebiotic to regulate health and metabolic changes via SCFAs production. Further studies are needed to explore new potential targets of GSPE in the modulation of metabolic endotoxemia and to

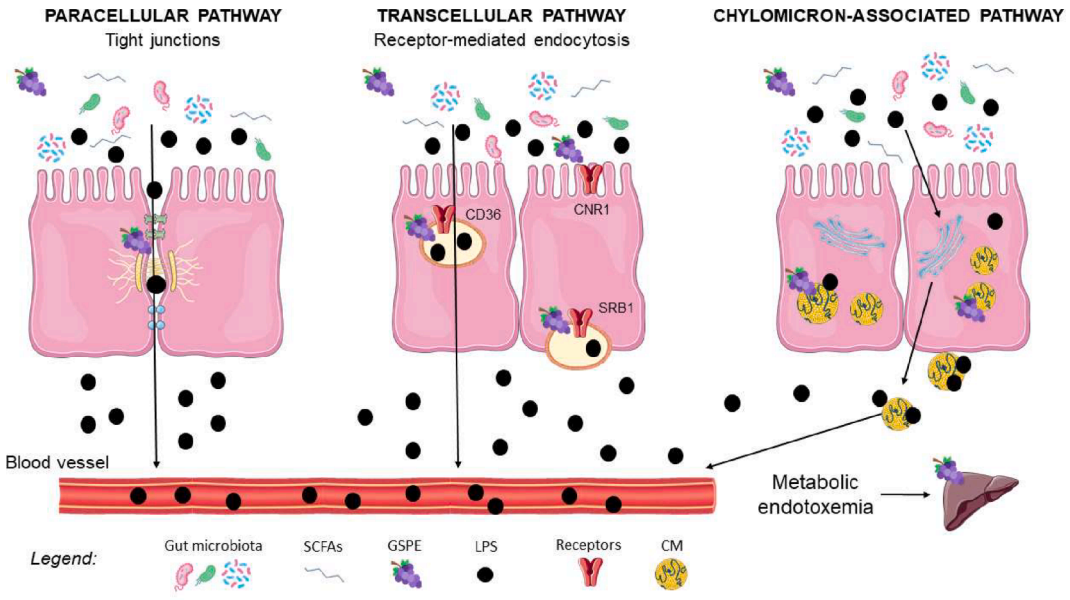

Fig. 7. LPS transport pathways across intestinal epithelial cells and proposed GSPE protective mechanisms. Consuming high-fat/high-sucrose diets provokes large changes in microbiota composition and function (dysbiosis), leading to the release and translocation of LPS through the intestinal barrier. The paracellular pathway permits LPS translocation by passive diffusion due to tight junction alterations; the transcellular pathway is mediated by specific scavenger receptors for dietary fatty acids such as CD36 and SRB1; and the lipoprotein-associated pathway permits LPS translocation through newly released chylomicrons during post-prandial period. LPS accumulation in blood circulation leads to metabolic endotoxemia and consequent inflammation of peripheral tissues, especially the liver. GSPE modulates metabolic endotoxemia via CNR1 by changing microbiota and SCFA profiles, *Cd36* and *Srb1* gene expression, affecting the metabolism of chylomicrons as well as reducing hepatic LPS accumulation. Abbreviations: *CD36, Cluster of Differentiation; CM, chylomicron; CNR1, Cannabinoid Receptor Type 1; GSPE, Grape Seed Proanthocyanidin Extract; LPS, lipopolysaccharide; SCFAs, short chain fatty acids; SRB1, Scavenger Receptor Class B Type 1.*

translate this to human nutrition.

Funding

This research was funded by MCIN/AEI/10.13039/501100011033/FEDER "Una manera de hacer Europa" AGL2017-83477-R and PID2021-122636OB-I00. M. Sierra-Cruz and A Miguéns-Gómez received a doctoral research grant from the Martí i Franquès programme of the Universitat Rovira i Virgili. M. Pinent and X. Terra are Serra Húnter fellows.

Author contributions

Marta Sierra-Cruz: Writing – original draft, Data curation, Methodology, Software. **Alba Miguéns-Gómez:** Methodology, Software. **Esther Rodríguez-Gallego:** Investigation, Conceptualization**. Claudio D'Addario**: Writing – review & editing. **Martina Di Bartolomeo**: epigenetic methodology. **M Teresa Blay:** Investigation, Conceptualization, Resources. **Montserrat Pinent**: Conceptualization, Funding acquisition, Project administration. **Raúl Beltrán-Debón**: Writing – review & editing, Formal analysis, Supervision. **Ximena Terra**: Writing – review & editing, Formal analysis, Supervision.

Declaration of Competing Interest

The authors declare that they have no known competing financial interests or personal relationships that could have appeared to influence the work reported in this paper.

Data availability

Data will be made available on request.

Acknowledgement

We would like to thank Niurka Llopiz for technical support.

References

Bladé, C., Aragonès, G., Arola-Arnal, A., Muguerza, B., Bravo, F. I., Salvadó, M. J., Arola, L., & Suárez, M. (2016). Proanthocyanidins in health and disease. *BioFactors, 42*(1), 5–12. https://doi.org/10.1002/biof.1249

Cabral, F., Al-Rahem, M., Skaggs, J., Thomas, T. A., Kumar, N., Wu, Q., Fadda, P., Yu, L., Robinson, J. M., Kim, J., Pandey, E., Sun, X., Jarjour, W. N., Rajaram, M. V. S., Harris, E. N., & Ganesan, L. P. (2021). Stabilin receptors clear LPS and control systemic inflammation. *IScience, 24*(11), Article 103337. https://doi.org/10.1016/j.isci.2021.103337

Cani, P. D., Amar, J., Iglesias, M. A., Poggi, M., Knauf, C., Bastelica, D., … Burcelin, R. (2007). Metabolic endotoxemia initiates obesity and insulin resistance. *Diabetes, 56*(7), 1761–1772. https://doi.org/10.2337/db06-1491

Casanova-Martí, À., Serrano, J., Portune, K. J., Sanz, Y., Blay, M. T., Terra, X., Ardévol, A., & Pinent, M. (2018). Grape seed proanthocyanidins influence gut microbiota and enteroendocrine secretions in female rats. *Food and Function, 9*(3), 1672–1682. https://doi.org/10.1039/c7fo02028g

Chen, M., Hou, P., Zhou, M., Ren, Q., Wang, X., Huang, L., Hui, S., Yi, L., & Mi, M. (2020). Resveratrol attenuates high-fat diet-induced non-alcoholic steatohepatitis by maintaining gut barrier integrity and inhibiting gut inflammation through regulation of the endocannabinoid system. *Clinical Nutrition, 39*(4), 1264–1275. https://doi.org/10.1016/j.clnu.2019.05.020

Clemente-Postigo, M., Oliva-Olivera, W., Coin-Aragüez, L., Ramos-Molina, B., Giraldez-Perez, R. M., Lhamyani, S., Alcaide-Torres, J., Perez-Martinez, P., El Bekay, R., Cardona, F., & Tinahone, F. J. (2019). Metabolic endotoxemia promotes adipose dysfunction and inflammation in human obesity. *American Journal of Physiology - Endocrinology and Metabolism, 316*(2), E319–E332. https://doi.org/10.1152/ajpendo.00277.2018

D'Addario, C., Zaplatic, E., Giunti, E., Pucci, M., Micioni Di Bonaventura, M. V., Scherma, M., Dainese, E., Maccarrone, M., Nilsson, I. A., Cifani, C., & Fadda, P. (2020). Epigenetic regulation of the cannabinoid receptor CB1 in an activity-based rat model of anorexia nervosa. *International Journal of Eating Disorders, 53*(5), 432–446. https://doi.org/10.1002/eat.23271

Damms-Machado, A., Louis, S., Schnitzer, A., Volynets, V., Rings, A., Basrai, M., & Bischoff, S. C. (2017). Gut permeability is related to body weight, fatty liver disease, and insulin resistance in obese individuals undergoing weight reduction. *American Journal of Clinical Nutrition, 105*(1), 127–135. https://doi.org/10.3945/ajcn.116.131110

Downing, L. E., Heidker, R. M., Caiozzi, G. C., Wong, B. S., Rodriguez, K., Del Rey, F., & Ricketts, M. L. (2015). A grape seed procyanidin extract ameliorates fructose-induced hypertriglyceridemia in rats via enhanced fecal bile acid and cholesterol excretion and inhibition of hepatic lipogenesis. *PLoS ONE, 10*(10). https://doi.org/10.1371/journal.pone.0140267

Engle, M. J., Goetz, G. S., & Alpers, D. H. (1998). Caco-2 cells express a combination of colonocyte and enterocyte phenotypes. In. *Journal of Cellular Physiology* (Vol. 174, Issue 3). https://doi.org/10.1002/(SICI)1097-4652(199803)174:3<362::AID-JCP10>3.0.CO;2-B

Ferraretto, A., Gravaghi, C., Donetti, E., Cosentino, S., Donida, B. M., Bedoni, M., Lombardi, G., Fiorilli, A., & Tettamanti, G. (2007). New methodological approach to induce a differentiation phenotype in Caco-2 cells prior to post-confluence stage. In. *Anticancer Research, 27*. Issue 6 B.

Fox, E. S., Thomas, P., & Broitman, S. A. (1990). Hepatic mechanisms for clearance and detoxification of bacterial endotoxins. *The Journal of Nutritional Biochemistry, 1*(12), 620–628. https://doi.org/10.1016/0955-2863(90)90020-L

Ge, Y., Ezzell, R. M., & Shaw Warren, H. (2000). Localization of endotoxin in the rat intestinal epithelium. *Journal of Infectious Diseases, 182*(3), 873–881. https://doi.org/10.1086/315784

Ghosh, S. S., Wang, J., Yannie, P. J., & Ghosh, S. (2020). Intestinal barrier dysfunction, LPS translocation, and disease development. *Journal of the Endocrine Society, 4*(2). https://doi.org/10.1210/jendso/bvz039

Ghoshal, S., Witta, J., Zhong, J., de Villiers, W., & Eckhardt, E. (2009). Chylomicrons promote intestinal absorption of lipopolysaccharides. *Journal of Lipid Research, 50*(1), 90–97. https://doi.org/10.1194/jlr.M800156-JLR200

Gil-Cardoso, K., Ginés, I., Pinent, M., Ardévol, A., Terra, X., & Blay, M. (2017). A cafeteria diet triggers intestinal inflammation and oxidative stress in obese rats. *British Journal of Nutrition, 117*(2), 218–229. https://doi.org/10.1017/S0007114516004608

Gil-Cardoso, K., Ginés, I., Pinent, M., Ardévol, A., Blay, M., & Terra, X. (2016). Effects of flavonoids on intestinal inflammation, barrier integrity and changes in gut microbiota during diet-induced obesity. *Nutrition Research Reviews, 29*(2), 234–248. https://doi.org/10.1017/S0954422416000159

Gil-Cardoso, K., Ginés, I., Pinent, M., Ardévol, A., Blay, M., & Terra, X. (2018). The co-administration of proanthocyanidins and an obesogenic diet prevents the increase in intestinal permeability and metabolic endotoxemia derived to the diet. *Journal of Nutritional Biochemistry, 62*, 35–42. https://doi.org/10.1016/j.jnutbio.2018.07.012

Ginés, I., Gil-Cardoso, K., Serrano, J., Casanova-Martí, À., Blay, M.t., Pinent, M., Ardévol, A., & Terra, X. (2018). Effects of an intermittent grape-seed proanthocyanidin (GSPE) treatment on a cafeteria diet obesogenic challenge in rats. *Nutrients, 10*(3). https://doi.org/10.3390/nu10030315

Ginés, I., Gil-Cardoso, K., Terra, X., Blay, M.t., Pérez-Vendrell, A. M., Pinent, M., & Ardévol, A. (2019). Grape Seed Proanthocyanidins target the enteroendocrine system in cafeteria-diet-fed Rats. *Molecular Nutrition and Food Research, 63*(11), 1–7. https://doi.org/10.1002/mnfr.201800912

Gnauck, A., Lentle, R. G., & Kruger, M. C. (2016). The characteristics and function of bacterial lipopolysaccharides and their endotoxic potential in humans. *International Reviews of Immunology, 35*(3), 189–218. https://doi.org/10.3109/08830185.2015.1087518

González-Quilen, C., Gil-Cardoso, K., Ginés, I., Beltrán-Debón, R., Pinent, M., Ardévol, A., Terra, X., & Blay, M. T. (2019). Grape-seed proanthocyanidins are able to reverse intestinal dysfunction and metabolic endotoxemia induced by a cafeteria diet in wistar rats. *Nutrients, 11*(5). https://doi.org/10.3390/nu11050979

González-Quilen, C., Rodríguez-Gallego, E., Beltrán-Debón, R., Pinent, M., Ardévol, A., Blay, M. T., & Terra, X. (2020). Health-promoting properties of proanthocyanidins for intestinal dysfunction. *Nutrients, 12*(1). https://doi.org/10.3390/nu12010130

Guerville, M., & Boudry, G. (2016). Gastrointestinal and hepatic mechanisms limiting entry and dissemination of lipopolysaccharide into the systemic circulation. *American Journal of Physiology - Gastrointestinal and Liver Physiology, 311*(1), G1–G15. https://doi.org/10.1152/ajpgi.00098.2016

Hayashi, H., Fujimoto, K., Cardelli, J. A., Nutting, D. F., Bergstedt, S., & Tso, P. (1990). Fat feeding increases size, but not number, of chylomicrons produced by small intestine. *In American Journal of Physiology - Gastrointestinal and Liver Physiology (Vol., 259*(5), 22–25. https://doi.org/10.1152/ajpgi.1990.259.5.g709

Hersoug, L. G., Møller, P., & Loft, S. (2016). Gut microbiota-derived lipopolysaccharide uptake and trafficking to adipose tissue: Implications for inflammation and obesity. *Obesity Reviews, 17*(4), 297–312. https://doi.org/10.1111/obr.12370

Jeyakumar, S. M., Vajreswari, A., & Giridharan, N. V. (2007). Impact of vitamin A on high-density lipoprotein-cholesterol and scavenger receptor class BI in the obese rat. *Obesity, 15*(2), 322–329. https://doi.org/10.1038/oby.2007.534

Kan, X., Liu, B., Guo, W., Wei, L., Lin, Y., Guo, Y., Gong, Q., Li, Y., Xu, D., Cao, Y., Huang, B., Dong, A., Ma, H., Fu, S., & Liu, J. (2019). Myricetin relieves LPS-induced mastitis by inhibiting inflammatory response and repairing the blood–milk barrier. *Journal of Cellular Physiology, 234*(9), 16252–16262. https://doi.org/10.1002/jcp.28288

Kim, K. A., Gu, W., Lee, I. A., Joh, E. H., & Kim, D. H. (2012). High fat diet-induced gut microbiota exacerbates inflammation and obesity in mice via the TLR4 signaling pathway. *PLoS ONE, 7*(10). https://doi.org/10.1371/journal.pone.0047713

Lenahan, C., Huang, L., Travis, Z. D., & Zhang, J. H. (2019). Scavenger Receptor Class B type 1 (SR-B1) and the modifiable risk factors of stroke. *Chinese Neurosurgical Journal, 5*(1). https://doi.org/10.1186/s41016-019-0178-3

Margalef, M., Pons, Z., Iglesias-Carres, L., Arola, L., Muguerza, B., & Arola-Arnal, A. (2016). Gender-related similarities and differences in the body distribution of grape

seed flavanols in rats. *Molecular Nutrition and Food Research, 60*(4), 760–772. https://doi.org/10.1002/mnfr.201500717

Moreno, D. A., Ilic, N., Poulev, A., Brasaemle, D. L., Fried, S. K., & Raskin, I. (2003). Inhibitory effects of grape seed extract on lipases. *Nutrition, 19*(10), 876–879. https://doi.org/10.1016/S0899-9007(03)00167-9

Morrison, D. J., & Preston, T. (2016). Formation of short chain fatty acids by the gut microbiota and their impact on human metabolism. *Gut Microbes, 7*(3), 189–200. https://doi.org/10.1080/19490976.2015.1134082

Muccioli, G. G., Naslain, D., Bäckhed, F., Reigstad, C. S., Lambert, D. M., Delzenne, N. M., & Cani, P. D. (2010). The endocannabinoid system links gut microbiota to adipogenesis. *Molecular Systems Biology, 6*, 392. https://doi.org/10.1038/msb.2010.46

Nauli, A. M., Sun, Y., Whittimore, J. D., Atyia, S., Krishnaswamy, G., & Nauli, S. M. (2014). Chylomicrons produced by Caco-2 cells contained ApoB-48 with diameter of 80–200 nm. *Physiological Reports, 2*(6), 1–12. https://doi.org/10.14814/phy2.12018

Pepino, M. Y., Kuda, O., Samovski, D., & Abumrad, N. A. (2014). Structure-function of CD36 and importance of fatty acid signal transduction in fat metabolism. *Annual Review of Nutrition, 34*, 281–303. https://doi.org/10.1146/annurev-nutr-071812-161220

Pons, Z., Guerrero, L., Margalef, M., Arola, L., Arola-Arnal, A., & Muguerza, B. (2014). Effect of low molecular grape seed proanthocyanidins on blood pressure and lipid homeostasis in cafeteria diet-fed rats. *Journal of Physiology and Biochemistry, 70*(2), 629–637. https://doi.org/10.1007/s13105-014-0329-0

Pucci, M., Micioni Di Bonaventura, M. V., Vezzoli, V., Zaplatic, E., Massimini, M., Mai, S., Sartorio, A., Scacchi, M., Persani, L., Maccarrone, M., Cifani, C., & D'Addario, C. (2019). Preclinical and clinical evidence for a distinct regulation of mu opioid and type 1 cannabinoid receptor genes expression in obesity. *Frontiers in Genetics, 10* (JUN), 523. https://doi.org/10.3389/fgene.2019.00523

Pucci, M., Zaplatic, E., Micioni Di Bonaventura, M. V., Micioni Di Bonaventura, E., De Cristofaro, P., Maccarrone, M., Cifani, C., & D'Addario, C. (2021). On the role of central type-1 Cannabinoid receptor gene regulation in food intake and eating behaviors. *International Journal of Molecular Sciences, 22*(1), 1–16. https://doi.org/10.3390/ijms22010398

Quesada, H., Del Bas, J. M., Pajuelo, D., Díaz, S., Fernandez-Larrea, J., Pinent, M., Arola, L., Salvadó, M. J., & Bladé, C. (2009). Grape seed proanthocyanidins correct dyslipidemia associated with a high-fat diet in rats and repress genes controlling lipogenesis and VLDL assembling in liver. *International Journal of Obesity, 33*(9), 1007–1012. https://doi.org/10.1038/ijo.2009.136

Quesada, H., Díaz, S., Pajuelo, D., Fernández-Iglesias, A., Garcia-Vallvé, S., Pujadas, G., Salvadó, M. J., Arola, L., & Bladé, C. (2012). The lipid-lowering effect of dietary proanthocyanidins in rats involves both chylomicron-rich and VLDL-rich fractions. *British Journal of Nutrition, 108*(2), 208–217. https://doi.org/10.1017/S0007114511005472

Ratajczak, W., Mizerski, A., Rył, A., Słojewski, M., Sipak, O., Piasecka, M., & Laszczyńska, M. (2021). Alterations in fecal short chain fatty acids (SCFAs) and branched short-chain fatty acids (BCFAs) in men with benign prostatic hyperplasia (BPH) and metabolic syndrome (MetS). *Aging, 13*(8), 10934–10954. https://doi.org/10.18632/aging.202968

Rohr, M. W., Narasimhulu, C. A., Rudeski-Rohr, T. A., & Parthasarathy, S. (2020). Negative effects of a high-fat diet on intestinal permeability: A Review. *Advances in Nutrition, 11*(1), 77–91. https://doi.org/10.1093/advances/nmz061

Salvadó, M. J., Casanova, E., Fernández-Iglesias, A., Arola, L., & Bladé, C. (2015). Roles of proanthocyanidin rich extracts in obesity. *Food and Function, 6*(4), 1053–1071. https://doi.org/10.1039/c4fo01035c

Sambuy, Y., De Angelis, I., Ranaldi, G., Scarino, M. L., Stammati, A., & Zucco, F. (2005). The Caco-2 cell line as a model of the intestinal barrier: Influence of cell and culture-related factors on Caco-2 cell functional characteristics. *Cell Biology and Toxicology, 21*(1), 1–26. https://doi.org/10.1007/s10565-005-0085-6

Sampey, B. P., Vanhoose, A. M., Winfield, H. M., Freemerman, A. J., Muehlbauer, M. J., Fueger, P. T., Newgard, C. B., & Makowski, L. (2011). Cafeteria diet is a robust model of human metabolic syndrome with liver and adipose inflammation: Comparison to high-fat diet. *Obesity, 19*(6), 1109–1117. https://doi.org/10.1038/oby.2011.18

Shi, Y., Jia, M., Xu, L., Fang, Z., Wu, W., Zhang, Q., Chung, P., Lin, Y., Wang, S., & Zhang, Y. (2019). miR-96 and autophagy are involved in the beneficial effect of grape seed proanthocyanidins against high-fat-diet-induced dyslipidemia in mice. *Phytotherapy Research, 33*(4), 1222–1232. https://doi.org/10.1002/ptr.6318

Sidibeh, C. O., Pereira, M. J., Lau Börjesson, J., Kamble, P. G., Skrtic, S., Katsogiannos, P., Sundbom, M., Svensson, M. K., & Eriksson, J. W. (2017). Role of cannabinoid receptor 1 in human adipose tissue for lipolysis regulation and insulin resistance. *Endocrine, 55*(3), 839–852. https://doi.org/10.1007/s12020-016-1172-6

Silva, Y. P., Bernardi, A., & Frozza, R. L. (2020). The role of short-chain fatty acids from gut microbiota in gut-brain communication. *Frontiers in Endocrinology, 11*. https://doi.org/10.3389/fendo.2020.00025

Smeriglio, A., Barreca, D., Bellocco, E., & Trombetta, D. (2017). Proanthocyanidins and hydrolysable tannins: Occurrence, dietary intake and pharmacological effects. *British Journal of Pharmacology, 174*(11), 1244–1262. https://doi.org/10.1111/bph.13630

Stephens, M., & von der Weid, P. Y. (2020). Lipopolysaccharides modulate intestinal epithelial permeability and inflammation in a species-specific manner. *Gut Microbes, 11*(3), 421–432. https://doi.org/10.1080/19490976.2019.1629235

Tedelind, S., Westberg, F., Kjerrulf, M., & Vidal, A. (2007). Anti-inflammatory properties of the short-chain fatty acids acetate and propionate: A study with relevance to inflammatory bowel disease. *World Journal of Gastroenterology, 13*(20), 2826–2832. https://doi.org/10.3748/wjg.v13.i20.2826

Tran, T. T. T., Poirier, H., Clément, L., Nassir, F., Pelsers, M. M. A. L., Petit, V., Degrace, P., Monnot, M. C., Glatz, J. F. C., Abumrad, N. A., Besnard, P., & Niot, I. (2011). Luminal lipid regulates CD36 levels and downstream signaling to stimulate chylomicron synthesis. *Journal of Biological Chemistry, 286*(28), 25201–25210. https://doi.org/10.1074/jbc.M111.233551

Venegas, D. P., De La Fuente, M. K., Landskron, G., González, M. J., Quera, R., Dijkstra, G., Harmsen, H. J. M., Faber, K. N., & Hermoso, M. A. (2019). Short chain fatty acids (SCFAs)mediated gut epithelial and immune regulation and its relevance for inflammatory bowel diseases. *Frontiers in Immunology, 10*(MAR), 277. https://doi.org/10.3389/fimmu.2019.00277

Yaman, S. O., Orem, A., Yucesan, F. B., Kural, B. V., & Orem, C. (2021). Evaluation of circulating miR-122, miR-30c and miR-33a levels and their association with lipids, lipoproteins in postprandial lipemia. *Life Sciences, 264*. https://doi.org/10.1016/j.lfs.2020.118585

Yao, M., Chen, J., Zheng, J., Song, M., McClements, D. J., & Xiao, H. (2013). Enhanced lymphatic transport of bioactive lipids: Cell culture study of polymethoxyflavone incorporation into chylomicrons. *Food and Function, 4*(11), 1662–1667. https://doi.org/10.1039/c3fo60335k

Yokooji, T., Nouma, H., & Matsuo, H. (2014). Characterization of ovalbumin absorption pathways in the rat intestine, including the effects of aspirin. In. *Biological and Pharmaceutical Bulletin* (Vol. 37, Issue 8). https://doi.org/10.1248/bpb.b14-00290